DOI: 10.1002/ejic.200700623

Syntheses, Crystal Structures, Thermal Stabilities, and Magnetic and Luminescent Properties of 3D Heterometal Phosphonates: $NaM[O_3PCH(OH)CO_2]$ (M = Mn, Fe, Co, Zn)

Zhuzhi Lai,[a] Ruibiao Fu,[a] Shengmin Hu,[a] and Xintao Wu*[a]

Keywords: Crystal structure / Phosphorus / Luminescence / Magnetism / Thermal stability

Four heterometal 2-hydroxyl(phosphono)carboxylates, $NaM[O_3PCH(OH)CO_2]$ [M = Mn (**1**), Fe (**2**), Co (**3**), Zn (**4**)], were synthesized hydrothermally. Single-crystal X-ray diffraction data reveal that they are isostructural and crystallize in the orthorhombic space group *Pbca* (No. 61) with a = 10.1365(16)–10.4557(5) Å, b = 9.6890(9)–9.8265(4) Å, c = 10.7942(19)–10.9353(1) Å, V = 1060.2(3)–1123.22(7) Å^3, and Z = 8. Each $[MO_6]$ (M = Mn, Fe, Co, Zn) octahedron contacts three neighboring $[NaO_5]$ pyramids through two edges and one corner to form a Na/MO layer. The layers are further connected by $O_3PCH(OH)CO_2^{3-}$ groups into an interesting 3D heterometallic framework. Thermogravimetric and powder X-ray diffraction analysis indicate that solids **1**–**4** are thermally stable up to 350, 250, 340, and 350 °C, respectively. Magnetic measurements show the presence of antiferromagnetic interaction for M^{II} ions (M = Mn, Fe, Co) in compounds **1**–**3**. These solids exhibit bright cyan (for **1**, **2**, and **4**) or purple (for **3**) luminescence after induced by fluorescent whitener, and the luminescence can be irreversibly transformed into bright yellow (for **1** and **4**) or red (for **3**) simply by annealing treatment at 300 °C.

Introduction

The design and construction of new inorganic–organic hybrid materials based on metal phosphonates is of current interest owing to their potential applications as catalysts, ion-exchangers, small molecular sensors, and nonlinear optics.[1] During the past two years, phosphonic acids containing a second functional group such as hydroxy, amine, carboxyl, and pyridyl, were successfully introduced as bridging ligands for the isolation of new metal phosphonates with intriguing structures and properties.[2–5] This is mainly due to the additional functional groups that can improve the solubility and crystallinity of metal phosphonates, which results in the growth of suitable single crystals for X-ray structural analysis. Then, an instinctive strategy of attaching two additional functional groups to the phosphonic acid was performed to obtain several novel solids, such as $M_x[Fe(O_2CCH_2)_2NCH_2PO_3]_6{\cdot}nH_2O$ (M = Na, K, Rb), with a maple leaf lattice and lanthanide phosphonates possessing homochiral porous frameworks as well as blue, red, or near IR luminescence.[6] In this regard, we focused on utilizing 2-hydroxy(phosphono)acetic acid (Hpaa) containing three functional groups (–OH,–COOH, and–PO_3H_2) to construct four-layered hybrid materials that are antiferromagnetic and one 3D polar open-framework with nonlinear optical activity and high thermal stability.[7] On one hand, there are few reports on heterometal phosphonates with multifunctional phosphonic acids as bridging groups.[6a,8] On the other hand, Hpaa would adopt numerous coordination modes through 6 active oxygen donors to bond a maximum of 15 metal atoms. Therefore, a series of experiments was carried out to search for new heterometallic polymers with Hpaa as bridging ligands. In this paper, we report the syntheses, structures, and properties (including thermal stability, magnetism, and luminescence) of four new heterometal phosphonates with a 3D framework, namely, $NaM[O_3PCH(OH)CO_2]$ (M = Mn: **1**; Fe: **2**; Co: **3**; Zn, **4**).

Results and Discussion

Syntheses and Characterization

Na_2L is a commercial fluorescent whitener; if it exists in the initial reaction mixture, the products are denoted as **1a**–**4a** and if not as **1b**–**4b**. Initially, the usage of **Na_2L** is to grow suitably sized single crystals of the metal phosphonates, because M^{2+}(M = Mn, Fe, Co, Zn) ions can be easily precipitated by **Na_2L**, which prevents the formation of large amounts of $NaM[O_3PCH(OH)CO_2]$ (M = Mn, Fe, Co, Zn). NH_4Cl may serve as a structure-directing agent to grow suitable single crystals. When NaF is treated with acetic acid, HF is produced, which can increase the solubility of

[a] State Key Laboratory of Structural Chemistry, Fujian Institute of Research on the Structure of Matter, Chinese Academy of Science,
Fuzhou, Fujian 350002, China
E-mail: wxt@fjirsm.ac.cn

Supporting information for this article is available on the WWW under http://www.eurjic.org or from the author.

these compounds and result in the growth of single crystals for X-ray structural analysis. Single crystals of these compounds can also be obtained without the salts or acetic acid. However, their size and quality are not suitable for single-crystal XRD.

Experimental powder XRD patterns of **1a**–**4a** are all consistent with those simulated from single-crystal X-ray data of compounds **1**–**4**, which indicates that final products **1a**–**4a** are homogeneous phases, and elemental analyses of **1a** and **3a** are in accord with the calculated values. Furthermore, the IR spectra of **1a** and **3a** are consistent with those of **2b** and **4b** and do not include absorption bands around 1198 and 1182 cm^{-1}, which are assigned to the asymmetric stretching vibrations of the sulfonate group (Supporting Information, Figure S1).[9] These results indicate that crystals of **1a** and **3a** that have been repeatedly rinsed with distilled water under ultrasonic treatment contain few residual Na_2L.

As shown in Figure S1 (Supporting Information), the IR spectra of **1a**, **2b**, **3a**, and **4b** have a medium band in the range of 3003–3049 cm^{-1}, which originates from the O–H stretching vibration of the hydroxy group. Additionally, a very strong band around 1590 cm^{-1} and a medium band near 1373 cm^{-1} are attributed to the carboxylate group. It is interesting that the P=O stretching vibration appears around 1176 cm^{-1}, which exhibits a redshift of about 24 cm^{-1} relative to those in [M{$HO_3PCH(OH)CO_2$}] (M = Mn, Fe, Co, Zn) and $(NH_4)Zn[O_3PCH(OH)CO_2]$.[7] Both diffuse reflectance spectra of compounds **3** and **3**–**300** have a broad and strong absorption band around 539 nm, which corresponds to the d–d transition of the Co^{II} ion (Supporting Information, Figure S2); the π–π* transitions of the C=O moiety for compounds **3** and **3**–**300** appear at 232 and 217 nm, respectively.

Structural Descriptions

Single-crystal XRD patterns revealed that compounds **1**–**4** are isostructural and feature a 3D heterometallic framework. In addition, all experimental powder XRD patterns of compounds **1**–**4** are in agreement with those simulated from single-crystal X-ray data of solid **1** (Figure 1). Therefore, only the structure of **1** will be discussed in detail as a representative. The asymmetric unit of **1** consists of one Mn^{II} ion, one Na^{I} ion, and one $O_3PCH(OH)CO_2^{3-}$ group (Figure 2). The $O_3PCH(OH)CO_2^{3-}$ group is chelated to the Mn^{II} ion through one phosphonate oxygen atom (O2a) and one carboxylate oxygen atom (O5) to form a Mn–O–C–C–P–O six-membered chelating ring; the Mn^{II} ion is also chelated by another equivalent $O_3PCH(OH)CO_2^{3-}$ group through the hydroxy group (O4c) and another carboxylate oxygen donor (O6) into a Mn–O–C–C–O five-membered chelating ring, which results in an obvious small bond angle [O4c–Mn1–O6 = 67.20(11)°]. This is similar to those in [M{$HO_3PCH(OH)CO_2$}] (M = Mn, Fe, Co, Zn).[7a] As a

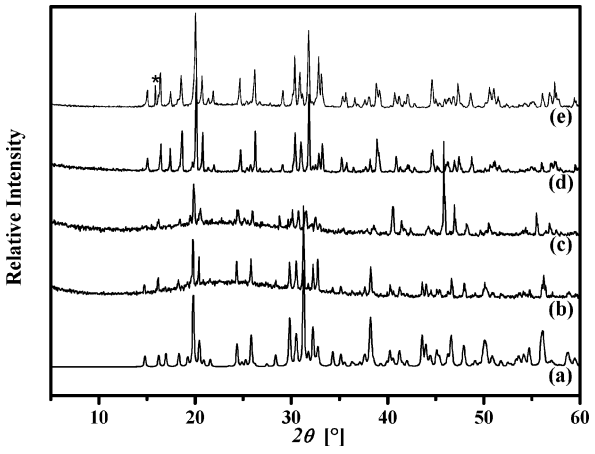

Figure 1. (a) The simulated XRD pattern of compound **1**; (b)–(e) experimental powder XRD patterns for compounds **1**–**4**, respectively. (*) The additional peak at about 15° may result from the background.

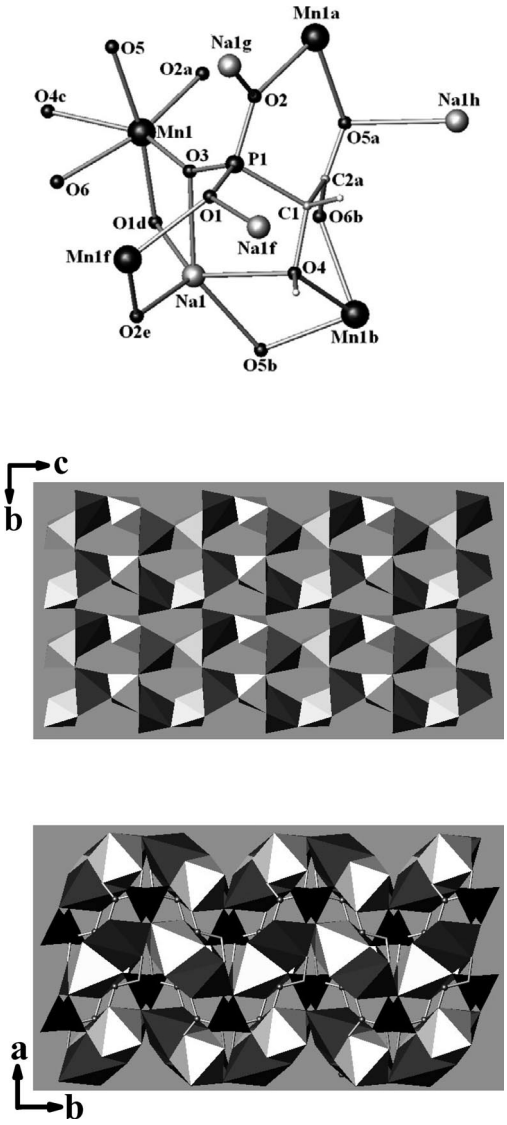

Figure 2. (Top) Ball–stick view of the coordination geometries of sodium, manganese, and phosphorus in compound **1**; (middle) polyhedral representation of the Na/MnO layer; and (bottom) 3D framework in compound **1**. White octahedron: [MnO_6], gray pyramid: [NaO_5], black tetrahedron: [CPO_3].

result, the Mn^{II} ion is located in a distorted [MnO_6] octahedral coordination geometry, which is completed by another two phosphonate oxygen atoms from two different equivalent $O_3PCH(OH)CO_2^{3-}$ groups (O1d and O3). The values of the Mn–O bond lengths are in the range of 2.198(3)–2.343(3) Å, whereas the Na^I geometry is a [NaO_5] pyramid, defined by three phosphonates oxygen atoms, one carboxylate oxygen donor, and one hydroxy group from four equivalent $O_3PCH(OH)CO_2^{3-}$ groups. The Na–O distances range from 2.349(3) to 2.485(3) Å. Except for O6b, which is only coordinated to one Mn^{II} ion, another oxygen atom of $O_3PCH(OH)CO_2^{3-}$ bonds one Mn^{II} ion and one Na^I ion. So, the $O_3PCH(OH)CO_2^{3-}$ group exhibits a new octadentate mode to combine four Mn^{II} ions and four Na^I ions. This is obviously different from the tetradentate mode in $(NH_4)Zn[O_3PCH(OH)CO_2]$ and the tridentate mode in $M[HO_3PCH(OH)CO_2]$ (M = Mn, Fe, Co, Zn).[7]

Each [MnO_6] octahedron shares two edges and one corner with neighboring three [NaO_5] pyramids, respectively, to form a Na/MnO layer consisting of six-membered rings (6MRs), and the Na/MnO layers are further bridged by $O_3PCH(OH)CO_2^{3-}$ groups and strong hydrogen bonds between –OH and –COO [O4–H2···O6$_{(x, -y-1/2, z+1/2)}$ = 2.632(4) Å] into an interesting 3D organic–inorganic hybrid framework.

Thermal Stabilities

Thermogravimetric analyses (TGA) of compounds **1**–**4** illustrate that under an atmosphere of nitrogen gas there is little weight loss for these compounds up to 410, 380, 390, and 370 °C, respectively (Figure 3). Thereupon, sharp weight-loss stages appear due to the decomposition of their frameworks. Furthermore, after solids **1**–**4** are annealed at 350, 250, 340 and 350 °C, respectively, their powder XRD patterns are all essentially in agreement with those simulated by single-crystal XRD data, which unambiguously indicate little change in their frameworks (Supporting Information, Figures S3–S6).

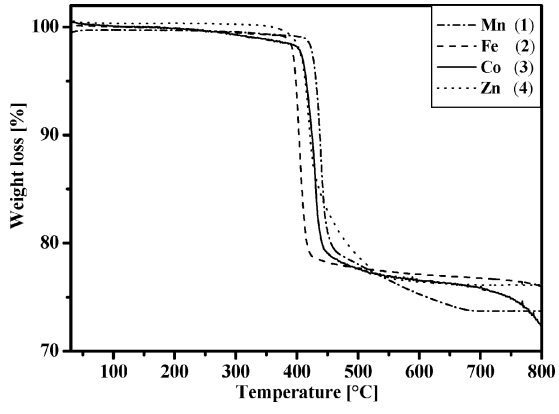

Figure 3. TGA curves of compounds **1**–**4**.

Magnetic Properties

The temperature dependence of the $\chi_m T$ product, magnetic susceptibility (χ_m) and inverse magnetic susceptibility ($1/\chi_m$) for compounds **1**–**3** at 5 kOe from 2 K to room temperature are shown in Figure S7 (Supporting Information).

The molar magnetic susceptibility of compound **1** increases with decreasing temperature and reaches a maximum at 5 K. At 305 K, the effective magnetic moment per manganese atom (5.70 μ_B) is consistent with the expected spin-only value of 5.92 μ_B (g = 2, S = 5/2), and also according to the reported magnetic moments of Mn^{II} ranging from 5.2 to 5.9 μ_B.[7] Upon cooling, $\chi_m T$ product decreases slowly from 305 to 50 K. Thereupon, $\chi_m T$ decreases more quickly to 1.41 emu K mol^{-1} at 2 K. In the temperature range of 2–305 K, the magnetic susceptibility follows the Curie–Weiss law [χ_m^{-1} = 1.82(5) + 0.2401(3)T] (r = 0.9999), with C = 4.16 emu K mol^{-1} and θ = –7.6 K. The above results demonstrate antiferromagnetic interaction of the Mn^{II} ions.[7a,10]

The effective magnetic moment per Fe^{II} ion (5.25 μ_B) for compound **2** at 307 K is slightly higher than the expected spin-only value of 4.90 μ_B (g = 2, S = 2).[10] With decreasing temperature, the effective magnetic moment decreases slowly down to 100 K (5.17 μ_B) and then rapidly to 2.75 μ_B at 2 K. Between 2 and 305 K, the magnetic susceptibility also fits well with the Curie–Weiss law [χ_m^{-1} = 1.28(2) + 0.2859(1)T] (r = 0.99999), with C = 3.50 emu K mol^{-1} and θ = –4.49 K. The decrease in the value of $\chi_m T$ with decreasing temperature and negative θ value indicate antiferromagnetic interaction of the Fe^{II} ions.[7a,10]

Unlike those of compounds **1** and **2**, the $\chi_m T$ product of **3** decreases gradually from 2.86 emu K mol^{-1} at 303 K down to 0.63 emu K mol^{-1} at 2 K. From the above-mentioned equation, at 303 K the effective magnetic moment per cobalt atom (μ_{eff} = 4.78 μ_B) is obviously higher than the reported spin-only value of 3.87 μ_B. However, the value lies in the range of 4.4–5.2 μ_B owing to orbital contribution at room temperature.[10] In the range of 10–303 K, the magnetic susceptibility is consistent with the Curie–Weiss law [χ_m^{-1} = 4.87(9) + 0.3362(6)T] (r = 0.9999), with C = 2.97 emu K mol^{-1} and θ = –14.5 K. The decrease in the value of $\chi_m T$ with decreasing temperature and negative θ value suggests antiferromagnetic interaction of the Co^{II} ion.[7a,10] In addition, the magnetic susceptibility and thermal dependence of the $\chi_m T$ product are almost in agreement with those of pristine solid after polycrystalline **3** was previously heated at 300 or 340 °C for 2 h in an air atmosphere (Supporting Information, Figure S8). This result indicates little change in the valence of cobalt during the annealing treatment.

Luminescent Properties

The solid-state luminescent properties of solids **1**–**4** were investigated under ambient temperature. Compounds **1b**–**4b** show no luminescence under our experimental conditions. In contrast, compounds **1a**–**4a** display bright blue-green (for **1a**, **2a** and **4a**) or purple (for **3a**) emission (Figure 4). The maximum band of **3a** is 434 nm, which exhibits a 11, 22, and 20-nm blueshift relative to those of compounds **1a**,

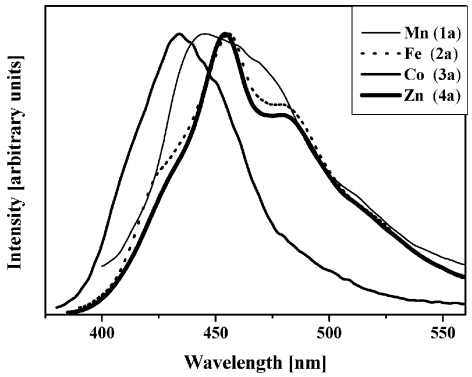

Figure 4. Normalized fluorescent emission spectra of **1a**–**4a** at room temperature in the solid state.

2a and **4a**, respectively. The blueshift is due to self-absorption through d–d transition of the Co^{II} ion in the range of 428–654 nm. These emissions cannot be attributed to MLCT (metal-to-ligand charge transfer) and LMCT (ligand-to-metal charge transfer) in nature, and may probably be assigned to the intraligand n–π* transition for two reasons: (1) a bright blue-green emission with λ_{max} = 460 nm can also be observed from a solution of (H_2O_3P)-$CH(OH)(CO_2H)$ and (2) all maximum bands of corresponding excitation spectra for solids **1a**–**4a** and (H_2O_3P)-$CH(OH)(CO_2H)$ solution fall in the range of 360–377 nm (Supporting Information, Figure S9, S10).[5] The lifetimes for $\lambda_{ex,em}$ = 380,450 nm of **1a** and $\lambda_{ex,em}$ = 368,460 nm of **2a** are 1.67(2) and 2.08(4) ns, respectively, which matches

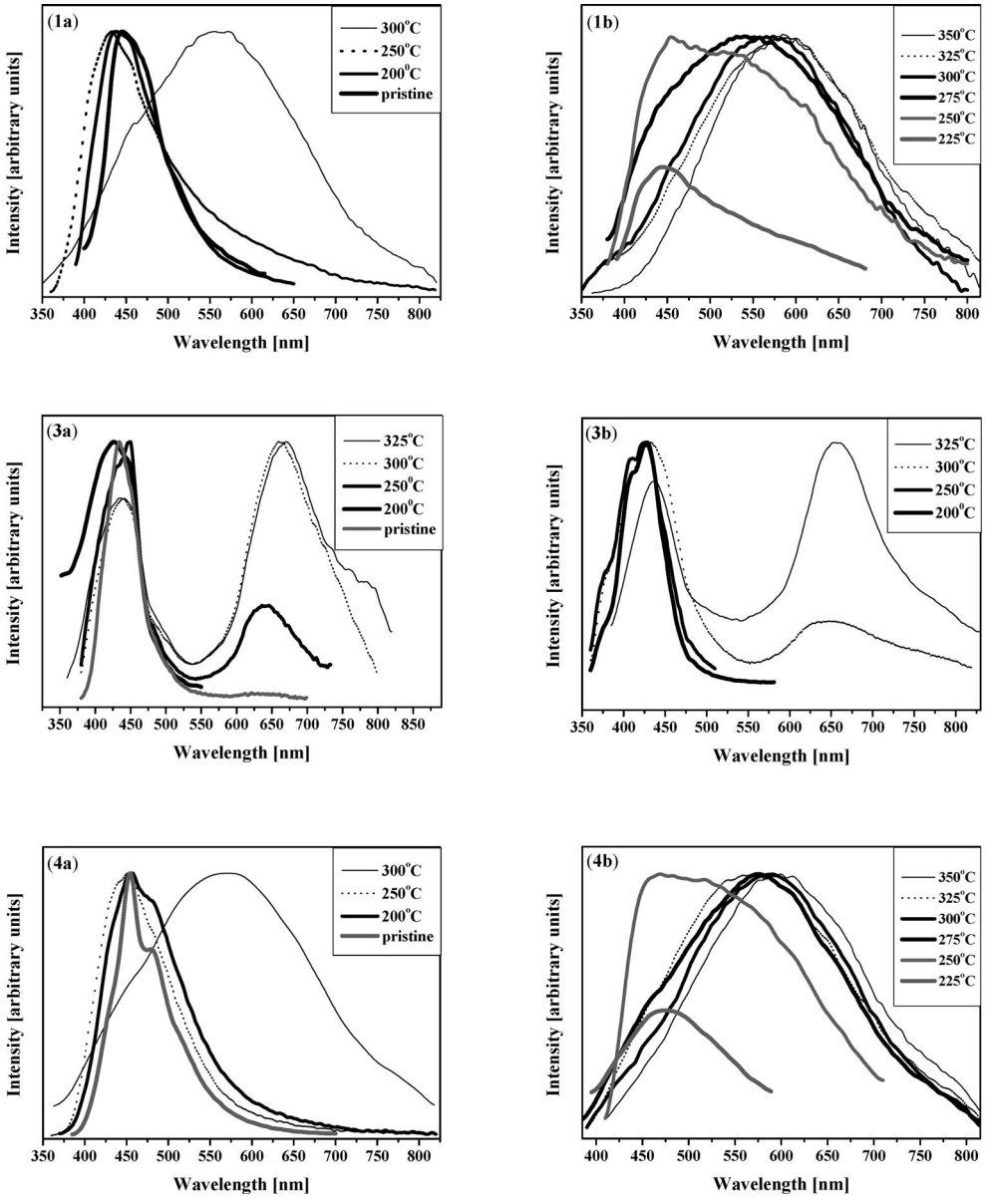

Figure 5. Room-temperature solid-state normalized fluorescent emission spectra of pristine **1a**, **1b**, **3a**, **3b**, **4a**, and **4b** − compounds were previously annealed at different temperatures.

that of Hpaa [2.69(5) ns for $\lambda_{ex,em}$ = 370,462 nm], whereas solid **3a** has a very short lifetime [0.35(2) ns, for $\lambda_{ex,em}$ = 352,430 nm]. Preliminary experimental results revealed that the luminescent intensities of **1a** and **3a** are about 16 and 27% of that of $\mathbf{Na_2L}$, respectively. Furthermore, it is surprising that if **3b** is previously immersed in dilute $\mathbf{Na_2L}$ solution for 6 d and then rinsed with distilled water under ultrasonic treatment repeatedly, it can also give off bright-purple luminescence similar to that of **3a** (Supporting Information, Figure S10). This phenomenon is also observed for **1b**. The above results indicate that $\mathbf{Na_2L}$ would induce intrinsic luminescence of **1**–**4**. However, the mechanism of how $\mathbf{Na_2L}$ induces the luminescence is still unknown. Furthermore, solid **3a** can also emit bright-purple luminescence if $\mathbf{Na_2L}$ is reduced to 0.01 mmol in the synthetic mixture, which indicates that the luminescent properties may not depend on the amount of $\mathbf{Na_2L}$ in the synthetic mixture. In addition, annealing treatment at 225 °C (for **1b** and **4b**) or 200–250 °C (for **3b**) can also induce weak blue-green (for **1b** and **4b**) and bright-purple (for **3b**) luminescence.

Another attractive feature of compounds **1**, **3**, and **4** is their irreversible transformation of luminescent color through annealing treatment (Figure 5). Both **1a** and **4a** will give off bright-yellow luminescence (λ_{max} = 571 nm) with a broad profile if they are previously annealed at 300 °C. The full width at half maximum heights (FWHM) of **1a** and **4a** are 239 and 258 nm, respectively. Because d–d transition for the Co^{II} ion would absorb blue and green light with a maximum at 539 nm, **3a** can emit both purple and red emissions after annealing treatment, which is different to those of **1a** and **4a**. The intensities of purple and red emissions for **3a** will be tuned with different annealing temperature. For example, if **3a** is previously annealed at 250 °C, it displays bright purplish red luminescence, and the intensity ratio between the two peak bands at 449 and 636 nm is –2.6. After **3a** is annealed at 300 °C, red luminescence is intensified to reduce the ratio between the two maximum bands at 440 and 659 nm to –0.78, resulting in bright-red emission. Noteworthy is that the luminescent spectra of **3a** that was previously annealed at 250 and 300 °C are similar to the absorption spectra of chlorophyll a and b, respectively, which indicates that **3a** is an attractive candidate to be used in light conversion agriculture materials [light conversion agriculture material has the function of converting a light spectrum (like UV, green light) into blue and red light so as to promote the growth of vegetables].

Similar transformations of luminescent color with annealing treatment can also be observed on solids **1b**, **3b**, and **4b**. Because the Mn^{II} ion is an important luminescent activator that gives off red emission, it seems that the transformation of luminescent colors for solids **1**, **3**, and **4** are not related to the transition-metal centers.[11] So, the IR spectra of solids **3** and **4** with different annealing temperatures were recorded to investigate the changes in the $O_3PCH(OH)CO_2^{3-}$ anion (Supporting Information, Figures S12, S13). However, all IR spectra are in agreement with those of the pristine solids. A suitable single crystal of **3** was carefully selected and annealed at 300 °C, and X-ray single-crystal diffraction revealed that the bond lengths of C=O and P–O in compound **3**–**300** are slightly shorter than those in pristine **3**, which results in the slight contraction of the unit-cell volume. This is in accord with the π–π* transition of C=O of compound **3**–**300**, which shows about a 15-nm blueshift relative to that of pristine **3** for strengthening the C=O band after the annealing treatment. Such slightly irreversible changes in the $O_3PCH(OH)CO_2^{3-}$ anion may cause the transformations of luminescent colors from blue-green to yellow (for **1**, **4**) or from purple to red (for **3**). In addition, the corresponding excitation spectra exhibit broad profiles in the range of 250–400 nm, which may be assigned to intraligand π–π* as well as n–π* transitions (Supporting Information, Figures S14–S19).

Furthermore, lifetimes for blue emission of solids **1** and **4** range from 1.6(1) to 3.21(7) ns, which are shorter than those of yellow emission [3.3(2)–6.3(4) ns] (Figures 6 and 7). For compound **3**, the lifetimes for purple and red luminescence are in the range of 0.35(4)–0.90(2) and 1.8(1)–2.7(2) ns, respectively (Figures 8 and 9).

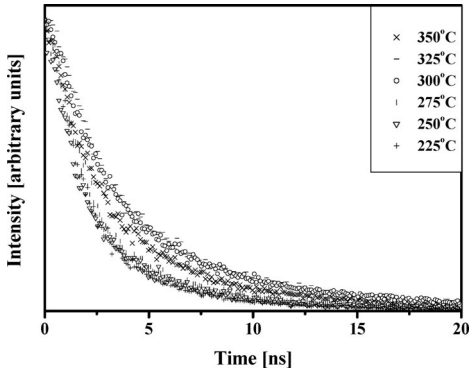

Figure 6. Room-temperature solid-state fluorescent intensity as a function of time for **1b** previously annealed at 225 ($\lambda_{ex,em}$ = 365, 445 nm), 250 ($\lambda_{ex,em}$ = 365, 420 nm), 275 ($\lambda_{ex,em}$ = 365, 458 nm), 300 ($\lambda_{ex,em}$ = 365, 575 nm), 325 ($\lambda_{ex,em}$ = 367, 580 nm), and 350 °C ($\lambda_{ex,em}$ = 370, 580 nm), respectively.

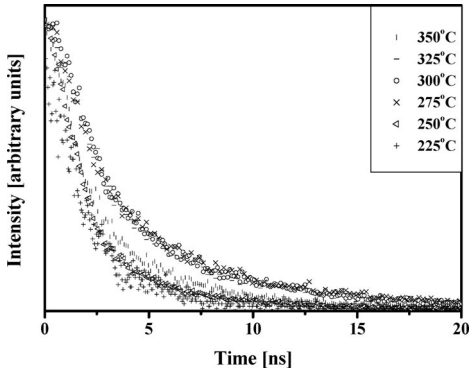

Figure 7. Room-temperature solid-state fluorescent intensity as a function of time for **4b** previously annealed at 225 ($\lambda_{ex,em}$ = 370, 478 nm), 250 ($\lambda_{ex,em}$ = 365, 460 nm), 275 ($\lambda_{ex,em}$ = 368, 573 nm), 300 ($\lambda_{ex,em}$ = 330, 588 nm), 325 ($\lambda_{ex,em}$ = 362, 562 nm), and 350 °C ($\lambda_{ex,em}$ = 365, 584 nm), respectively.

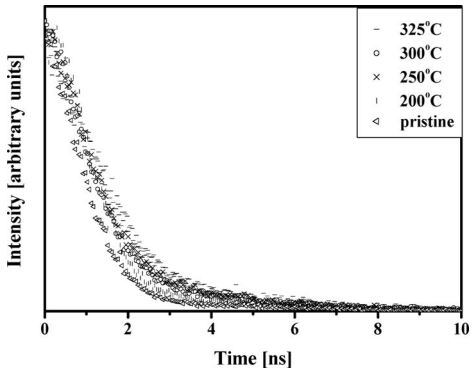

Figure 8. Room-temperature solid-state fluorescent intensity as a function of time for **3a** ($\lambda_{ex,em}$ = 352, 430 nm) as well as **3a** previously annealed at 200 ($\lambda_{ex,em}$ = 350, 428 nm), 250 ($\lambda_{ex,em}$ = 330, 445 nm), 300 ($\lambda_{ex,em}$ = 340, 440 nm), and 325 °C ($\lambda_{ex,em}$ = 362, 436 nm), respectively.

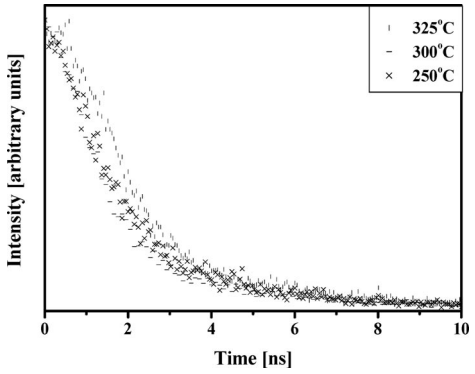

Figure 9. Room-temperature solid-state fluorescent intensity as a function of time for **3a** previously annealed at 250 ($\lambda_{ex,em}$ = 360, 640 nm), 300 ($\lambda_{ex,em}$ = 340, 660 nm), and 325 °C ($\lambda_{ex,em}$ = 365, 668 nm), respectively.

Conclusions

In summary, the hydrothermal syntheses, crystal structures, and properties (including thermal stability, magnetism, and luminescence) of four new heterometal 2-hydroxyl-(phosphono)carboxylates were described. Solids **1**, **3**, and **4** are the first phosphonate-based compounds that possess intrinsic blue-green or purple luminescence properties induced by fluorescent whitener (**Na_2L**) or heat treatment. The luminescent colors can be irreversibly transformed into yellow or red emission by simple annealing treatment. These properties make them of interest for potential application as emitters in displaying technology, as well as advanced anticounterfeiting technical products.

Experimental Section

Materials and Instrumentation: Hydroxy(phosphono)acetic acid solution was obtained from Changzhou City Jianghai Chemical Factory as water treatment agent (48.0 wt.-%). All other chemicals were obtained from commercial sources and used without further purification. Compounds **1**–**4** were synthesized in 25-mL Teflon-lined stainless steel vessels under autogenous pressure. The reactants were stirred homogeneously before heating. Elemental analyses were carried out with a Vario EL III element analyzer. Infrared spectra were obtained with a Nicolet Magna 750 FTIR spectrometer. The diffuse reflectance spectra of compounds **3** and **3**–**300** (polycrystalline **3** was previously annealed at 300 °C for 2 h in an air atmosphere) were recorded with a Perkin–Elmer Lambda 35 UV/Vis spectrometer. Fluorescent properties of solids **1**–**4** were investigated with FLS920 and LifeSpec-ps at ambient temperature. Thermogravimetric analysis was performed with a NETZSCH STA449C under nitrogen gas flow at a heating rate of 10 °C min^{-1} (for **1** and **4**) or 15 °C min^{-1} (for **2** and **3**) from room temperature to 800 °C. Powder X-ray diffraction (XRD) patterns were acquired with a DMAX-2500 diffractometer by using Cu-K_α radiation in an ambient environment. Magnetic properties of compounds **1**–**3** were measured with a Quantum Design PPMS at a magnetic field of 5000 Oe from 2 K to room temperature.

$NaMn[O_3PCH(OH)CO_2]$ (1): A mixture of $Mn(CH_3COO)_2{\cdot}4H_2O$ (0.2536 g, 1.035 mmol), disodium 4,4′-bis(2-sulfonatostiryl)biphenyl (**Na_2L**; 0.5821 g, 1.035 mmol), NH_4Cl (2.2102 g, 41.32 mmol), NaF (0.0904 g, 2.153 mmol), $(H_2O_3P)CH(OH)(CO_2H)$ solution (0.5 mL, 2 mmol), and H_2O (10.0 mL) was heated at 140 °C for 96 h. The final mixture was repeatedly rinsed with distilled water under ultrasonic treatment to obtain pure colorless crystals of **1**. Experimental powder XRD pattern of the product was in agreement with that simulated from single-crystal X-ray data, which indicated a homogeneous phase. The yield was 67% (0.1594 g) based on $Mn(CH_3COOH)_2{\cdot}4H_2O$. Final pH value of this reaction mixture was 3.72. $C_2H_2MnNaO_6P$ (230.94): calcd. C 10.40, H 0.87; found C 10.63, H 1.24. IR (KBr pellet): $\tilde{\nu}$ = 999 (w), 999 (vs, υas_{CO}), 999 (s), 3049 (m, υ_{O-H}), 2929 (w, υ_{C-H}), 2786 (w), 2733 (w), 2625 (w), 2520 (w), 1589 (vs, υas_{CO}), 1423 (s, δ_{C-H}), 1373 (m, υs_{CO}), 1273 (m, δ_{C-H}), 1176 (s, $\upsilon_{P=O}$), 1144 (s, υ_{P-O}), 1095 (vs, υ_{P-O}), 1056 (w, υ_{P-O}), 995 (m, υ_{P-O}), 983 (w), 847 (w), 796 (m), 767 (w, υ_{C-P}), 748 (w, υ_{C-P}), 665 (w), 588 (m), 542 (m), 494 (s) cm^{-1}. Crystals of **1** can also be obtained in the absence of **Na_2L** and NH_4Cl as follows: A mixture of $Mn(CH_3COO)_2{\cdot}4H_2O$ (0.1225 g, 0.4998 mmol), NaF (0.3500 g, 8.335 mmol), $(H_2O_3P)CH(OH)(CO_2H)$ solution (1.0 mL, 4 mmol), acetic acid (2.0 mL), and H_2O (8.0 mL) was heated at 120 °C for 144 h. The final mixture was also rinsed with distilled water under ultrasonic treatment many times to obtain pure colorless crystals of **1**. Experimental powder XRD pattern of the product was in accord with that simulated from single-crystal X-ray data, which indicated a homogeneous phase.

$NaFe[O_3PCH(OH)CO_2]$ (2): A mixture of $FeCl_2{\cdot}4H_2O$ (0.1014 g, 0.5100 mmol), NH_4Cl (2.5 g, 47 mmol), NaF (0.4 g, 9.5 mmol), $(H_2O_3P)CH(OH)(CO_2H)$ solution (0.7 mL, 3 mmol), and H_2O (10.0 mL) was heated at 140 °C for 96 h. The final mixture was repeatedly rinsed with distilled water under ultrasonic treatment to obtain pure colorless crystals of **2**. Experimental powder XRD pattern of the product was in agreement with that simulated from single-crystal X-ray data, which indicated a homogeneous phase. The yield was 33% (0.0383 g) based on $FeCl_2{\cdot}4H_2O$. Final pH value of this reaction mixture was 3.79. $C_2H_2FeNaO_6P$ (231.85): calcd. C 10.36, H 0.87; found C 10.32, H 1.16. IR (KBr pellet): $\tilde{\nu}$ = 3026 (m, υ_{O-H}), 2931 (w, υ_{C-H}), 2786 (w), 2733 (w), 2625 (w), 2524 (w), 1591 (vs, υas_{CO}), 1426 (s, δ_{C-H}), 1374 (s, υs_{CO}), 1275 (s, δ_{C-H}), 1177 (s, $\upsilon_{P=O}$), 1148 (s, υ_{P-O}), 1088 (vs, υ_{P-O}), 1056 (w, υ_{P-O}), 993 (s, υ_{P-O}), 985 (s), 845 (m), 806 (m), 773 (w, υ_{C-P}), 753 (w, υ_{C-P}), 665 (m), 594 (m), 549 (m), 490 (s) cm^{-1}. Crystals of **2** can also be obtained with **Na_2L** in an initial mixture as follows: A mixture of $FeCl_2{\cdot}4H_2O$ (0.1001 g, 0.5035 mmol), **Na_2L** (0.2801 g, 0.4980 mmol), NaF (0.4001 g, 9.528 mmol), $(H_2O_3P)CH(OH)(CO_2H)$ solution (1 mL, 4 mmol), acetic acid (2.0 mL), and

H_2O (8.0 mL) was heated at 120 °C for 144 h The final mixture was also rinsed with distilled water under ultrasonic treatment many times to obtain pure crystals of **2** Experimental powder XRD pattern of the product was also in agreement with that simulated from single-crystal X-ray data, which indicated a homogeneous phase.

$NaCo[O_3PCH(OH)CO_2]$ (3): A mixture of $Co(CH_3COO)_2{\cdot}4H_2O$ (0.249 g, 1.00 mmol), **Na_2L** (0.5843 g, 1.039 mmol), NaF (0.1657 g, 3.946 mmol), $(H_2O_3P)CH(OH)(CO_2H)$ solution (0.7 mL, 3 mmol), acetic acid (2.0 mL), and H_2O (8.0 mL) was heated at 140 °C for 96 h. The final mixture was repeatedly rinsed with distilled water under ultrasonic treatment to obtain pure red crystals of **3**. Experimental powder XRD pattern of the product was in agreement with that simulated from single-crystal X-ray data, which indicated a homogeneous phase. The yield was 93% (0.2172 g) based on $Co(CH_3COOH)_2{\cdot}4H_2O$. Final pH value of this reaction mixture was 3.80. $C_2H_2CoNaO_6P$ (234.93): calcd. C 10.23, H 0.86; found C 10.26, H 1.22. IR (KBr pellet): $\tilde{\nu}$ = 3003 (m, υ_{O-H}), 2936 (m, υ_{C-H}), 2787 (w), 2729 (w), 2619 (w), 2521 (w), 1595 (vs, υas_{CO}), 1428 (s, δ_{C-H}), 1373 (m, υs_{CO}), 1273 (m, δ_{C-H}), 1177 (s, $\upsilon_{P=O}$), 1151 (s, υ_{P-O}), 1090 (vs, υ_{P-O}), 1054 (w, υ_{P-O}), 987 (vs, υ_{P-O}), 846 (m), 813 (m), 777 (w, υ_{C-P}), 756 (w, υ_{C-P}), 671 (m), 660 (m), 593 (m), 557 (m), 492 (s) cm^{-1}. Crystals of **3** can also be obtained in the absence of **Na_2L** as follows: A mixture of $Co(CH_3COO)_2{\cdot}4H_2O$ (0.249 g, 1.00 mmol), NaF (0.2001 g, 4.765 mmol), (H_2O_3P)-$CH(OH)(CO_2H)$ solution (0.5 mL, 2 mmol), acetic acid (0.5 mL), and H_2O (8.0 mL) was heated at 120 °C for 144 h. The final mixture was also rinsed with distilled water under ultrasonic treatment many times to obtain pure red crystals of **3**. Experimental powder XRD pattern of the product was also in agreement with that simulated from single-crystal X-ray data, which indicated a homogeneous phase.

$NaZn[O_3PCH(OH)CO_2]$ (4): A mixture of $Zn(CH_3COO)_2{\cdot}2H_2O$ (0.11 g, 0.501 mmol), NaF (0.35 g, 8.3 mmol), $(H_2O_3P)CH$-$(OH)(CO_2H)$ solution (1.0 mL, 4 mmol), acetic acid (2.0 mL), and H_2O (8.0 mL) was heated at 140 °C for 96 h. The final mixture was repeatedly rinsed with distilled water under ultrasonic treatment to obtain pure crystals of **4**. Experimental powder XRD pattern of the product was in agreement with that simulated from single-crystal X-ray data, which indicated a homogeneous phase. The yield was 46% (0.0490 g) based on $Zn(CH_3COO)_2{\cdot}2H_2O$. Final pH value of this reaction mixture was 2.84. $C_2H_2NaO_6PZn$ (241.37): calcd. C 9.95, H 0.84; found C 9.95, H 1.24. IR (KBr pellet): $\tilde{\nu}$ = 3023 (m, υ_{O-H}), 2935 (w, υ_{C-H}), 2792 (w), 2737 (w), 2625 (w), 2524 (w), 1591 (vs, υas_{CO}), 1433 (s, δ_{C-H}), 1376 (s, υs_{CO}), 1277 (m, δ_{C-H}), 1179 (s, $\upsilon_{P=O}$), 1154 (s, υ_{P-O}), 1083 (vs, υ_{P-O}), 1062 (w, υ_{P-O}), 994 (s, υ_{P-O}), 985 (w), 848 (m), 808 (m), 776 (w, υ_{C-P}), 755 (w, υ_{C-P}), 673 (m), 663 (m), 594 (m), 558 (m), 500 (s), 490 (s) cm^{-1}. Crystals of **4** can also be obtained with **Na_2L** in an initial mixture as follows: A mixture of $Zn(CH_3COO)_2{\cdot}2H_2O$ (0.2195 g, 1.000 mmol), NaF (0.2001 g, 4.765 mmol), **Na_2L** (0.5602 g, 0.9960 mmol), (H_2O_3P)-$CH(OH)(CO_2H)$ solution (0.5 mL, 2 mmol), acetic acid (0.5 mL), and H_2O (8.0 mL) was heated at 140 °C for 96 h. The final mixture was rinsed with distilled water under ultrasonic treatment many times to obtain pure crystals of **4**. Experimental powder XRD pattern of the product was also in agreement with that simulated from single-crystal X-ray data, which indicated a homogeneous phase.

Single-Crystal X-ray Diffraction: X-ray data were collected at 293(2) K with a Siemens SMART-CCD diffractometer (for **1**), a Rigaku Mercury CCD/AFC diffractometer (for **2**–**4**), and a Saturn 70 CCD diffractometer (for **3**–**300**) by using graphite-monochromated Mo-K_α radiation [λ(Mo-K_α) = 0.71073 Å]. Data of compound **1** were reduced and absorption corrected with SMART and SADABS software, respectively, whereas data of compounds **2**–**4** and **3**–**300** were reduced with CrystalClear v1.3. These structures were solved by direct methods and refined by full-matrix least-squares techniques on F^2 by using SHELXTL-97.[12] All non-hydrogen atoms were treated anisotropically. The positions of hydrogen atoms were located from difference Fourier map and assigned with fixed isotropic thermal parameter. Crystal data are summarized in Table 1. CCDC-629750 to -629753 for compounds **1**–**4**, respectively, contain the supplementary crystallographic data for this paper. These data can be obtained free of charge from The Cambridge Crystallographic Data Centre via www.ccdc.cam.ac.uk/data_request/cif.

Relative Luminescent Intensity: Coin-like tablets of solids **1a**, **3a**, and **Na_2L** with about 1.3-cm diameter and 0.1-cm thickness were prepared at room temperature. First, a tablet of **Na_2L** was excited at 372 nm to obtain the emission spectrum, and then all the experimental conditions (including optical set up, focalization point, illuminated cross-section, sample holder, and emission and excitation slits width) were held constant and a tablet of solid **1a** was excited at 376 nm to obtain the emission spectrum. Second, a tablet of **Na_2L** was excited at 410 nm to obtain the emission spectrum, and then all the experimental conditions (including optical set up, focalization point, illuminated cross-section, sample holder, and emis-

Table 1. Crystallographic data for compounds **1**–**4**.

Complex	**1**	**2**	**3**	**3-300**	**4**
Formula	$C_2H_2MnNaO_6P$	$C_2H_2FeNaO_6P$	$C_2H_2CoNaO_6P$	$C_2H_2CoNaO_6P$	$C_2H_2ZnNaO_6P$
FW	230.94	231.85	234.93	234.93	241.37
Space group	*Pbca*	*Pbca*	*Pbca*	*Pbca*	*Pbca*
a [Å]	10.4557(5)	10.266(3)	10.1998(9)	10.181(3)	10.1365(16)
b [Å]	9.8265(4)	9.743(3)	9.6890(9)	9.673(3)	9.6893(15)
c [Å]	10.9353(1)	10.862(3)	10.7943(10)	10.784(3)	10.7942(19)
V [Å^3]	1123.22(7)	1086.3(5)	1066.76(17)	1062.1(5)	1060.2(3)
Z	8	8	8	8	8
T [K]	293(2)	293(2)	293(2)	293(2)	293(2)
$D_{calcd.}$ [g cm^{-3}]	2.731	2.835	2.926	2.938	3.024
μ [mm^{-1}]	2.682	3.119	3.566	3.582	4.984
GOF on F^2	1.168	1.101	1.185	1.111	1.307
R_{int}	0.0230	0.0190	0.0368	0.0208	0.0500
$R1$[a] [$I > 2\sigma(I)$]	0.0455	0.0202	0.0341	0.0173	0.0444
$wR2$[b] [all data]	0.1189	0.0493	0.0643	0.0446	0.0832

[a] $R1 = \Sigma(||F_o| - |F_c||)/\Sigma |F_o|$. [b] $wR2 = \{\Sigma w[(F_o^2 - F_c^2)]/\Sigma w[(F_o^2)^2]\}^{0.5}$.

sion and excitation slits width) were held constant and a tablet of solid **3a** was excited at 352 nm to obtain the emission spectrum.

Annealing Treatment: In an oven, polycrystallines of **1**–**4** were heated in air from room temperature to the required temperature over 30 min and then held at that temperature for 120 min. The crystals were then naturally cooled to ambient temperature.

Supporting Information (see also the footnote on the first page of this article): Tables of selected bond lengths and angles and plots consisting of IR, PXRD, magnetic, and luminescent data.

Acknowledgments

This research was supported by grants from the State Key Laboratory of Structure Chemistry, Fujian Institute of Research on the Structure of Matter, Chinese Academy of Sciences (CAS), the National Ministry of Science and Technology of China (2007CB815301 and 2006CB932900), the National Science Foundation of China (20733003 and 20673118), the Science Foundation of CAS, and Fujian Province for Research Funding Support (KJCX2-YW-M05, 2005HZ01-1, 2007J0171, 2006J0014 and 2006F3132).

[1] a) A. Clearfield, "Metal Phosphonate Chemistry" in *Progress in Inorganic Chemistry* (Eds.: A. D. Karlin), John Wiley & Sons, New York, **1998**, vol. 47, pp. 371–510; b) A. Clearfield in *New Developments in Ion Exchange Materials* (Eds.: M. Abe, T. Kataoka, T. Suzuki), Kodansha, Ltd., Tokyo, **1991**; c) I. O. Benítez, B. Bujoli, L. J. Camus, C. M. Lee, F. Odobel, D. R. Talham, *J. Am. Chem. Soc.* **2002**, *124*, 4363–4370; d) G. E. Fanucci, J. Krzystek, M. W. Meisel, L.-C. Brunel, D. R. Talham, *J. Am. Chem. Soc.* **1998**, *120*, 5469–5479; e) C. Y. Ortiz-Avila, C. Bhardwaj, A. Clearfield, *Inorg. Chem.* **1994**, *33*, 2499–2500; f) T. E. Mallouk, J. A. Gavin, *Acc. Chem. Res.* **1998**, *31*, 209–217; g) L. C. Brousseau III, T. E. Mallouk, *Anal. Chem.* **1997**, *69*, 679–687; h) O. R. Evans, W. Lin, *Acc. Chem. Res.* **2002**, *35*, 511–522; i) K. Maeda, *Microporous Mesoporous Mater.* **2004**, *73*, 47–54; j) A. Clearfield, Z. Wang, *J. Chem. Soc. Dalton Trans.* **2002**, 2937–2947; k) A. Clearfield, *Curr. Opinion. Sol. State Mater. Res.* **2002**, *6*, 495–506.

[2] a) B. Liu, P. Yin, X. Y. Yi, S. Gao, L. M. Zheng, *Inorg. Chem.* **2006**, *45*, 4205–4213; b) B. Liu, Y. Z. Li, L. M. Zheng, *Inorg. Chem.* **2005**, *44*, 6921–6923; c) X. Y. Yi, B. Liu, R. Jiménez-Aparicio, F. A. Urbanos, S. Gao, W. Xu, J. S. Chen, Y. Song, L. M. Zheng, *Inorg. Chem.* **2005**, *44*, 4309–4314; d) P. Yin, S. Gao, Z. M. Wang, C. H. Yan, L. M. Zheng, X. Q. Xin, *Inorg. Chem.* **2005**, *44*, 2761–2765.

[3] a) J. A. Groves, S. R. Miller, S. J. Warrender, C. Mellot-Draznieks, P. Lightfoota, P. A. Wright, *Chem. Commun.* **2006**, 3305–3307; b) J. Kratochvil, M. Necas, V. Petricek, J. Pinkas, *Inorg. Chem.* **2006**, *45*, 6562–6564; c) R. Vivani, F. Costantino, U. Costantino, M. Nocchetti, *Inorg. Chem.* **2006**, *45*, 2388–2390; d) S. S. Bao, G. S. Chen, Y. Wang, Y. Z. Li, L. M. Zheng, Q. H. Luo, *Inorg. Chem.* **2006**, *45*, 1124–1129; e) S. Bauer, H. Mu1ller, T. Bein, N. Stock, *Inorg. Chem.* **2005**, *44*, 9464–9470; f) J. A. Groves, P. A. Wright, P. Lightfoot, *Inorg. Chem.* **2005**, *44*, 1736–1739; g) B. P. Yang, J. G. Mao, *Inorg. Chem.* **2005**, *44*, 566–571; h) J. A. Groves, S. R. Miller, S. J. Warrender, C. Mellot-Draznieks, P. Lightfoota, P. A. Wright, *Chem. Commun.* **2006**, 3305–3307; i) C. Serre, J. A. Groves, P. Lightfoota, A. M. Z. Slawin, P. A. Wright, N. Stock, T. Bein, M. Haouas, F. Taulelle, G. Férey, *Chem. Mater.* **2006**, *18*, 1451–1457; j) K. Abu-Shandi, H. Winkler, C. Janiak, *Z. Anorg. Allg. Chem.* **2006**, *632*, 629–633; k) K. Abu-Shandi, C. Janiak, *Z. Naturforsch., Teil B* **2005**, *60*, 1250–1254.

[4] a) X. M. Zhang, J. J. Hou, W. X. Zhang, X. M. Chen, *Inorg. Chem.* **2006**, *45*, 8120–8125; b) J. Svoboda, V. Zima, L. Beneš, K. Melánová, M. Vlček, *Inorg. Chem.* **2005**, *44*, 9968–9976; c) M. M. Gómez-Alcantara, M. A. G. Aranda, P. Olivera-Pastor, P. Beran, J. L. García-Muñoz, A. Cabeza, *Dalton Trans.* **2006**, 577–585.

[5] a) X. M. Gan, B. M. Rapko, J. Fox, I. Binyamin, S. Pailloux, E. N. Duesler, R. T. Paine, *Inorg. Chem.* **2006**, *45*, 3741–3745; b) S. Comby, R. Scopelliti, D. Imbert, L. Charbonnière, R. Ziessel, J. C. G. Bu1nzli, *Inorg. Chem.* **2006**, *45*, 3158–3160.

[6] a) D. Cave, F. C. Coomer, E. Molinos, H. H. Klauss, P. T. Wood, *Angew. Chem. Int. Ed.* **2006**, *45*, 803–806; b) Q. Yue, J. Yang, G. H. Li, G. D. Li, J. S. Chen, *Inorg. Chem.* **2006**, *45*, 4431–4439; c) J. L. Song, J. G. Mao, *Chem. Eur. J.* **2005**, *11*, 1417–1424; d) Y. Gong, W. Tang, W. B. Hou, Z. Y. Zha, C. W. Hu, *Inorg. Chem.* **2006**, *45*, 4987–4995; e) D. K. Cao, Y. Z. Li, Y. Song, L. M. Zheng, *Inorg. Chem.* **2005**, *44*, 3599–3604; f) D. K. Cao, Y. Z. Li, L. M. Zheng, *Inorg. Chem.* **2005**, *44*, 2984–2985.

[7] a) R. B. Fu, S. C. Xiang, H. S. Zhang, J. J. Zhang, X. T. Wu, *Cryst. Growth Des.* **2005**, *5*, 1795–1799; b) R. B. Fu, H. S. Zhang, L. S. Wang, S. M. Hu, Y. M. Li, X. H. Huang, X. T. Wu, *Eur. J. Inorg. Chem.* **2005**, 3211–3213.

[8] P. Vojtíšek, P. Cígler, J. Kotek, J. Rudovský, P. Hermann, I. Lukeš, *Inorg. Chem.* **2005**, *44*, 5591–5599.

[9] J. M. Kesselman-Truttmann, S. J. Hug, *Environ. Sci. Technol.* **1999**, *33*, 3171–3176.

[10] a) F. Sanz, C. Parada, J. M. Rojo, C. Ruiz-Valero, *Chem. Mater.* **2001**, *13*, 1334–1340; b) R. l. Carlin, *Magneto-Chemistry*, Springer, New York, **1986**.

[11] a) Y. B. Dong, G. X. Jin, M. D. Smith, R. Q. Huang, B. Tang, H. C. zur Loye, *Inorg. Chem.* **2002**, *41*, 4909–4914; b) X. D. Guo, G. S. Zhu, Q. R. Fang, M. Xue, G. Tian, J. Y. Sun, X. T. Li, S. L. Qiu, *Inorg. Chem.* **2005**, *44*, 3850–3855; c) J. Tao, M. L. Tong, J. X. Shi, X. M. Chen, S. W. Ng, *Chem. Commun.* **2000**, 2043–2044; d) M. García-Hipólito, O. Alvarez-Fregoso, E. Martínez, C. Falcony, M. A. Aguilar-Frutis, *Optic. Mater.* **2002**, *20*, 113–118; e) J. Wang, S. B. Wang, Q. Su, *J. Mater. Chem.* **2004**, *14*, 2569–2574.

[12] G. M. Sheldrick, *SHELXT 97: Program for Crystal Structure Refinement*, University of Göttingen, Germany, **1997**.

Received: June 15, 2007
Published Online: October 8, 2007

